Permeability of Granular Soils through LBM-DEM Coupling

N.M. Phan
Postgraduate Research Student, Centre for Geomechanics and Railway Engineering (CGRE), and ITTC-Rail, University of Wollongong, Australia

B. Indraratna
Distinguished Professor, and Director of Transport Research Centre (TRC), Faculty of Engineering and Information Technology (FEIT), University of Technology Sydney (UTS), Australia

T.T. Nguyen
Research Fellow, Transport Research Centre (TRC), School of Civil and Environmental Engineering, FEIT, University of Technology Sydney (UTS), Australia

ABSTRACT: Permeability of granular soils is one of the important factors when designing foundation as it affects the seepage, stability, and settlement of the foundation. The traditional methods such as experimental and analytical approaches can measure this parameter, however, they become inaccurate when soil properties such as porosity and particle distribution vary during fluid flowing. Therefore, computational methods which can capture both particle and fluid behaviours, and their mutual interactions have received greater attention in recent years. This paper presents a novel numerical approach where fluid variables are coupled with particles to predict hydraulic behaviours. While the particle behaviour can be captured by the Discrete Element Method (DEM) using Newton's second law, the fluid dynamics behaviour will be described by the Lattice Boltzmann Method (LBM) based on a distribution function. The mutual interaction between these two phases is carried out so that particle and fluid variables are updated constantly. The numerical results are validated with experiments showing a good agreement.

1 INTRODUCTION

The permeability of porous materials is a fundamental parameter in the geotechnical field as it can be used for designing the seepage, drainage and many other associated geotechnical purposes. For example, the hydraulic behaviour plays an important role in discharge capacity of natural fibre drains where the porous characteristics are very complex (Nguyen et al. 2018; Nguyen and Indraratna 2019). These characteristics can be measured by traditional methods such as experiments or analytical approaches. However, these methods are lack of the ability to capture the fluid behavior at microscopic level such as localized fluid variables in the porous media. In addition, micro-parameters such as the particle shape and size can have significant influences on the macro-hydraulic conductivity (Nguyen and Indraratna 2017b; Nguyen and Indraratna 2020c), thus more rigorous approach to predict the hydraulic properties of geomaterials is needed. As a result, numerical approaches which can capture the particle and fluid interactions at the microscopic level have been received greater attention in recent years (Tsuji et al. 1993; Kloss et al. 2012; Nguyen and Indraratna 2020b).

This study uses the Discrete Element Method (DEM) coupled with Lattice Boltzmann method (LBM) which is an alternative approach to the conventional Computational Fluid Dynamics (CFD) methods based on Navier-Stoke (NS) equations, to model the permeability of granular soil. Despite considerable success in using CFD-DEM coupling to model hydraulic behaviour of geomaterials, previous studies (Nguyen and Indraratna 2017a, 2020a) also indicate limited accuracy when using NS method to capture microscopic properties of fluid flows. For example, a common numerical technique is using the coarse-grid approach for the CFD-DEM coupling that restricts the scale of predicted fluid variables to the size of particles. LBM, in comparison with conventional CFD, demonstrates a higher degree of resolution as well as the ability to model complex geometries (Feng et al. 2007; Han and Cundall 2013; Indraratna et al. 2021), which is why it is used in this current study.

2 THEORIETICAL BACKGROUND

2.1 *Discrete Element Method*

The DEM was first introduced in (Cundall and Strack 1979) and has been widely used in geotechnical field to model the granular soil, especially at the micromechanical scale. The method uses Newton's Law to calculate particle translational and rotational motion as follows:

$$m_i \frac{dU_{p,i}}{dt} = \sum_{n_c} F_{c,ij} + F_{f,i} + F_{g,i} \quad (1)$$

$$I_i \frac{d\omega_i}{dt} = \sum_{n_c} T_{c,ij} + T_{f,i} \quad (2)$$

where m_i and I_i are the mass and moment of inertia, $U_{p,i}$ and ω_i are the translational and angular velocities, and $T_{c,ij}$ and $T_{f,i}$ are the torques exerting on particle due to other particles and fluid, respectively. F_{cij} is the contact force between adjacent particles. $F_{f,i}$ is the total fluid–particle force interacting on particle. $F_{g,i}$ is the gravitational force. n_c is the total number of contacts.

To simulate particle contact, this current study uses the non-linear contact model which combines Hertz and Mindlin-Deresiewicz theory. This model has been used widely to model particle contact of granular materials with significant success. How to compute contact forces can be found in previous studies (Zhu et al. 2007; Nguyen and Indraratna 2020b)

2.2 *Lattice Boltzmann Method*

The theories of LBM have been thoroughly explained through previous studies (Zou and He 1997; Chen and Doolen 1998; Feng et al. 2007; Krüger et al. 2009). The following section summarizes the important fundamental theory of LBM.

LBM is an immersing alternative method to the conventional CFD solver based on Navier Stoke equation. While the conventional CDF methods are based on using of average fluid variables which leads to less accuracy, LBM has been successful in modelling complex fluid flow such as flow through porous media and multiphase flows (Succi et al. 1989; Aidun and Clausen 2009). Unlike convention CFD using the Navier-Stokes equation to directly solve the macroscopic quantity such as the velocity and pressure, the LBM describes fluid as fluid density distribution function (FDDF) $f_i(x,t)$ moving along the lattice node. This movement involves two consecutive steps streaming and collision. Streaming is the process that $f_i(x,t)$ moves from the current node (x) to the neighbour node (x+$e_i\Delta_t$) at the lattice velocity c and in the direction of the lattice velocity vector e_i (Table 1). Since D3Q19 structure is adopted in this study, the FDDFs are split into 18 directional components (Figure 1). At the new node, the FDDFs are collided and get bouncing back in the opposite direction.

$$\underbrace{f_i(x + e_i\Delta_t, t + \Delta t)}_{streaming} = \underbrace{f_i(x,t) - \frac{1}{\tau}\left(f_i^{eq}(x,t) - f_i(x,t)\right)}_{collision} \quad (3)$$

where Δt the lattice time, τ is the relaxation time and f_i^{eq} is the equilibrium distribution which is computed by:

$$f_i^{eq} = w_i \rho_f \left(1 + \frac{3}{c^2} e_i U_{f,i} + \frac{9}{2c^4}\left(e_i U_{f,i}\right)^2 - \frac{3}{2c^2} U_{f,i}^2\right) \quad (4)$$

in which w_i is the weighting factor shown in Table 1. ρ_f and $U_{f,i}$ are the fluid density and velocity.

The macroscopic observables like density, velocity and pressure can directly be recovered by

$$\rho_f = \sum_{i=0}^{18} f_i \quad (5)$$

$$\vec{U}_f = \frac{1}{\rho_f} \sum_{i=0}^{18} f_i e_i \quad (6)$$

$$P_f = C_s^2 \rho_f \quad (7)$$

where C_s is the fluid speed of sound. $C_s = c/\sqrt{3}$; c = Δx/Δt (Δx is lattice spacing).

The kinematic viscosity of fluid can be determined by the relaxation time:

$$\nu = \frac{1}{3}\left(\tau - \frac{1}{2}\right)\frac{\Delta x^2}{\Delta t} \quad (8)$$

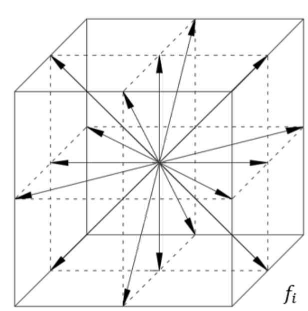

Figure 1: D3Q19 lattice model

From Equation (7), the relaxation time needs to be larger than 0.5 to ensure the viscosity is positive. Given that the stability of LBM model is sensitive to the relaxation time and Mach number. To keep the simulation under the incompressible limit, Mach number needs to be smaller than 0.1

$$M_a = \frac{U_{f,max}}{C_s} \quad (9)$$

Table 1: The velocity vector and weighting factor of D3Q19 model

i	Lattice velocity vector, e_i	Weight, w_i
$i = 0$	(0,0,0)	1/3
i = 1,..6	$(\pm c, 0, 0), (0, \pm c, 0), (0, 0, \pm c)$	1/18
i = 7,.18	$(\pm c, \pm c, 0), (\pm c, 0, \pm c), (0, \pm c, \pm c)$	1/36

2.3 *LBM-DEM coupling through Immerse Moving Boundary*

In this study, the Immerse Moving Boundary (IMB) proposed by (Noble and Torczynski 1998), is used to consider fluid-solid interaction. This method is widely used to simulate the particle moving in fluid (Feng et al. 2007). The advantage of this boundary is that it considers both solid and fluid in a lattice cell. As a result, it reduces the fluctuation of forces acting on the particles (Feng et al. 2007).

This method introduces a modified collision operator for the fluid nodes that are partially or fully occupied by solid. Equation (3) becomes:

$$f_i(x + e_i\Delta_t, t, +\Delta t) - f_i(x,t) = -\frac{1}{\tau}(1 - B)\left(f_i(x,t) - f_i^{eq}(x,t)\right) + B\Omega_i^s \quad (10)$$

where B is the weighting function and can be calculated by:

$$B(\varepsilon, \tau) = \frac{\varepsilon\left(\tau - \frac{1}{2}\right)}{(1-\varepsilon) + \left(\tau - \frac{1}{2}\right)} \quad (11)$$

in which ε is the solid ratio in the lattice cell

And the new additional collision term can be computed by:

$$\Omega_i^s = f_{-i}(x,t) - f_i(x,t) + f_i^{eq}(\rho_f, U_p) - f_{-i}^{eq}(\rho_f, U_f) \quad (12)$$

where U_p is the solid particle velocity

The hydrodynamic force and torques exerting on particles can be computed by:

$$F_f = \sum_{n_s} B_{n_s} \sum_i \Omega_i^s e_i \quad (13)$$

$$T_f = \sum_{n_s} (x_{n_s} - x_c) \times \left(B_{n_s} \sum_i \Omega_i^s e_i\right) \quad (14)$$

where n_s is the number of lattice cells covered by the solid particle, and x_c and x_{ns} are the centroid of the solid particle and the lattice node, respectively.

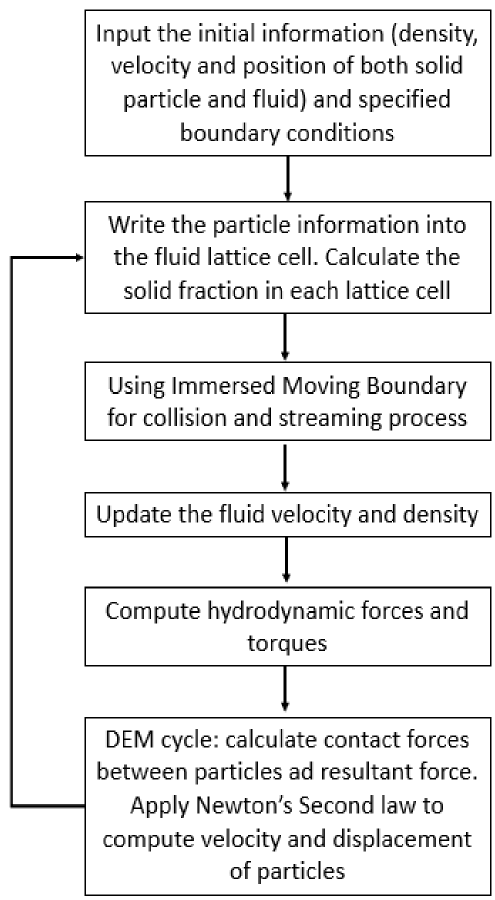

Figure 2: Flow diagram for LBM-DEM coupling algorithms

To sum up, in LBM-DEM numerical model, the LBM exerts the hydrodynamic forces on particles in DEM. If these forces are larger than the body weight of the particles, the particles start to move. Newton's Second Law is applied to determine these movements. The new particle position and orientation are continuously updated and written into the lattice to determine the solid ratio in the lattice cell. Using the modified collision proposed by IBM, the new hydrodynamic force and torque can be computed. The loop continues until simulation time finishes (Figure 2).

3 EXPERIMENT AND NUMERICAL SETUP

In this study, the numerical results are validated with the results obtained from the experiments conducted in this current and a previous studies (Fleshman and Rice 2014). The uniform coarse sand is used for the validation.

3.1 *Experiment*

Figure 3 shows the experimental setup. The permeability of the soil sample can be obtained by:

$$k_T = \frac{QL}{Aht} \tag{15}$$

where Q is the volume of collected water, L is the height of sample, A is sample cross section, h is the water head difference and t is interval time.

The steady flow is established to the inlet at the bottom and the water discharge is collected at the outlet at the top. The water head difference is measured by the manometers. A thin filter layer is laid at the bottom to ensure the uniform water distribution. Further details of the test can be found in other publication of the authors (Indraratna et al. 2021).

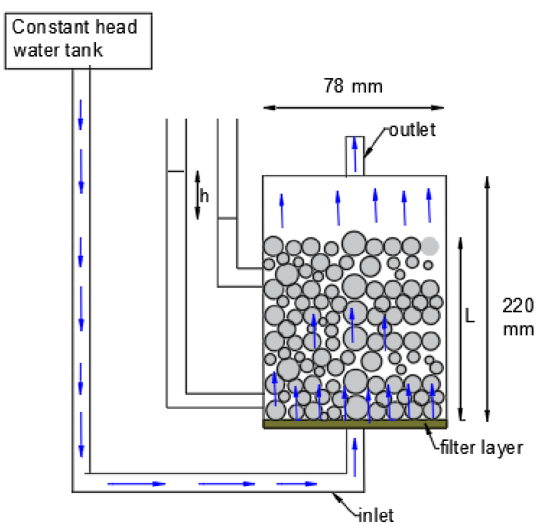

Figure 3: Experimental setup for permeability test

3.2 *Numerical model*

Soil sample having a similar PSD to the experimental sample is generated in DEM. The soil properties are adopted from previous studies (Kafui et al. 2002; Zeghal and El Shamy 2008; Nguyen and Indraratna 2020a) as shown in Table 2.

In this model, the pressure difference is applied at the inlet and outlet. And the discharge velocity (V_d) is obtained. The permeability in the numerical model can be computed by:

$$k = \frac{V_d}{i} \tag{16}$$

where i is the hydraulic gradient

$$i = \frac{\Delta P_f}{\rho g \Delta L} \tag{17}$$

in that ΔP_f is the pressure drop and ΔL is the distance that the fluid travels through soil.

Table 2: Soil and fluid parameters used in this current numerical investigation

Parameters	**Value**	**Unit**
Particles		
Specific gravity	2.65	
Young modulus	6.1×10^5	kPa
Coefficient of friction	0.5	
Coefficient of restitution	0.3	
Poisson's ratio	0.4	
Fluid		
Density	1000	kg/m^3
Kinematic viscosity	10^{-6}	m^2/s

4 RESULTS AND DISCUSSION

4.1 *Permeability*

In this section, the permeability captured by the numerical simulation is validated with experiment result and previous study which has the comparable properties and particle size distribution (PSD) with the soil used in this model. The range of porosity is from 0.39 to 0.46. Overall, the experiment shows a good agreement between numerical and experimental results (Table 3). The deviations between numerical and experimental results are small, which are 18.9% compared with the current experiment and 11.2% compared with the previous study. Such differences occur due to the difference in cell friction and particle shape. Besides that, the test also proves that the higher the porosity, the higher the permeability.

Table 3: Permeability of soil with different porosities and approaches

	Experiment (Current study)	Numerical results	Experiment (Fleshman and Rice 2014)	Numercial result
Porosity	0.39	0.39	0.45	0.46
Permeability (m/s)	0.0037	0.0044	0.0089	0.0079

4.2 *Localized fluid variables*

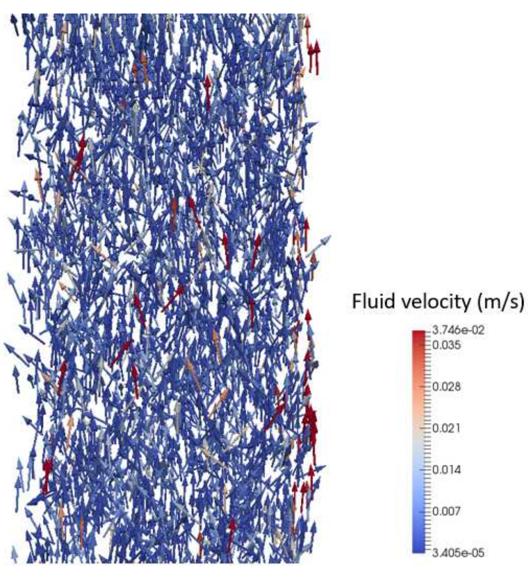

Figure 4: Interstitial micro-fluid vector flowing through particle bed

The advantage of using numerical simulation over the traditional method is the ability to capture localized variables of fluid over detailed porous properties. For instance, the laboratory test can capture the average fluid flow through particle bed, however, it is difficult or almost impossible to measure the local velocity of fluid flowing through the pore space. The arrows in Figure 4 demonstrate the fluid flow through the particle bed. The fluid velocity does not distribute uniformly showing by different colors of the arrows, which due to the different size of the pore. Fundamentally, fluid flow through larger pore has the slower velocity than fluid flow through smaller pore. In addition, it also illustrates that due to the solid obstacles, the fluid can only flow through the gap between particles, therefore, the fluid vectors do not in parallel with each other.

5 CONCLUSION

A study based on LBM-DEM coupling was carried out to investigate the permeability of granular materials. The numerical model represented in this paper showed certain success in predicting hydraulic properties of granular materials. Following conclusions could be highlighted:

The LBM-DEM numerical model can reasonably predict the permeability of the granular soil with different porosities. The deviation between numerical model and experiment is acceptable, from 11.2% to 18.9%. The numerical model can also capture very well the porosity-dependent behaviour of hydraulic conductivity that is understandable well through past experiments.

The fluid-particle coupling based on LBM can capture the localized fluid velocity as well as show how the fluid flows through the porous medium of granular soils. The results showed that the velocity of fluid flowing through the particle bed varies significantly with the localized characteristics of porous systems.

ACKNOWLEDGMENTS

This research was supported by the Australian Government through the Australian Research Council's Linkage Projects funding scheme (project LP160101254) and the Industrial Transformation Training Centre for Advanced Technologies in Rail Track Infrastructure (ITTC), University of Wollongong. The financial and technical supports from SMEC, Coffey, ACRI, Sydney Trains and ARTC (Australian Rail Track Corporation) are acknowledged

REFERENCES

Aidun, C. and Clausen, J. 2009. Lattice-Boltzmann Method for Complex Flows. *Annual Review of Fluid Mechanics*, **42**: 439-472. doi: 10.1146/annurev-fluid-121108-145519.

Chen, S. and Doolen, G.D. 1998. Lattice Boltzmann Method For Fluid Flows. *Annual Review of Fluid Mechanics*, **30**(1): 329-364. doi: 10.1146/annurev.fluid.30.1.329.

Cundall, P.A. and Strack, O.D.L. 1979. A discrete numerical model for granular assemblies. *Géotechnique*, **29**(1): 47-65. doi: 10.1680/geot.1979.29.1.47.

Feng, Y.T., Han, K. and Owen, D.R.J. 2007. Coupled lattice Boltzmann method and discrete element modelling of particle transport in turbulent fluid flows: Computational issues. *International Journal for Numerical Methods in Engineering*, **72**(9): 1111-1134. doi: 10.1002/nme.2114.

Fleshman, M.S. and Rice, J.D. 2014. Laboratory Modeling of the Mechanisms of Piping Erosion Initiation. *Journal of Geotechnical and Geoenvironmental Engineering*, **140**(6): 04014017. doi: 10.1061/(ASCE)GT.1943-5606.0001106.

Han, Y. and Cundall, P.A. 2013. LBM–DEM modeling of fluid–solid interaction in porous media. *International Journal for Numerical and Analytical Methods in Geomechanics*, **37**(10): 1391-1407. doi: 10.1002/nag.2096.

Indraratna, B., Phan, N.M., Nguyen, T.T. and Huang, J. 2021. Simulating Subgrade Soil Fluidization Using LBM-DEM Coupling. *International Journal of Geomechanics*, **21**(5): 04021039. doi: doi:10.1061/(ASCE)GM.1943-5622.0001997.

Kafui, K.D., Thornton, C. and Adams, M.J. 2002. Discrete particle-continuum fluid modelling of gas–solid fluidised beds. *Chemical Engineering Science*, **57**(13): 2395-2410.

Kloss, C., Goniva, C., Hager, A., Amberger, S. and Pirker, S. 2012. Models, algorithms and validation for opensource DEM and CFD-DEM. Vol. 12.

Krüger, T., Varnik, F. and Raabe, D. 2009. Shear stress in lattice Boltzmann simulations. *Physical review. E, Statistical, nonlinear, and soft matter physics*, **79**: 046704. doi: 10.1103/PhysRevE.79.046704.

Nguyen, T.T. and Indraratna, B. 2017a. Experimental and numerical investigations into hydraulic behaviour of coir fibre drain. *Canadian Geotechnical Journal*, **54**(1): 75-87. doi: 10.1139/cgj-2016-0182.

Nguyen, T.T. and Indraratna, B. 2017b. The permeability of natural fibre drains, capturing their micro-features. *Proceedings of the Institution of Civil Engineers - Ground Improvement*, **170**(3): 123-136. doi: 10.1680/jgrim.16.00032.

Nguyen, T.T. and Indraratna, B. 2019. Micro-CT scanning to examine soil clogging behavior of natural fiber drains. *ASCE Journal of Geotechnical and Geoenvironmental Engineering*, **145**(9): 04019037. doi: 10.1061/(ASCE)GT.1943-5606.0002065.

Nguyen, T.T. and Indraratna, B. 2020a. A coupled CFD-DEM approach to examine the hydraulic critical state of soil under increasing hydraulic gradient. *ASCE International Journal of Geomechanics*, **20**(9): 04020138-1:15. doi: https://doi.org/10.1061/(ASCE)GM.1943-5622.0001782.

Nguyen, T.T. and Indraratna, B. 2020b. The energy transformation of internal erosion based on fluid-particle coupling. *Computers and Geotechnics*, **121**: 103475. doi: https://doi.org/10.1016/j.compgeo.2020.103475.

Nguyen, T.T. and Indraratna, B. 2020c. The role of particle shape on hydraulic conductivity of granular soils captured through Kozeny–Carman approach. *Géotechnique Letters*, **10**(3): 398-403. doi: 10.1680/jgele.20.00032.

Nguyen, T.T., Indraratna, B. and Carter, J. 2018. Laboratory investigation into biodegradation of jute drains with implications for field behaviour. *ASCE Journal of Geotechnical & Geoenvironmental Engineering*, **144**(6): 04018026-1:15. doi: https://doi.org/10.1061/(asce)gt.1943-5606.0001885.

Noble, D.R. and Torczynski, J.R. 1998. A Lattice-Boltzmann Method for Partially Saturated Computational Cells. *International Journal of Modern Physics C*, **09**(08): 1189-1201. doi: 10.1142/S0129183198001084.

Succi, S., Foti, E. and Higuera, F. 1989. Three-Dimensional Flows in Complex Geometries with the Lattice Boltzmann Method. *Europhysics Letters (EPL)*, **10**(5): 433-438. doi: 10.1209/0295-5075/10/5/008.

Tsuji, Y., Kawaguchi, T. and Tanaka, T. 1993. Discrete particle simulation of two-dimensional fluidized bed. *Powder Technology*, **77**(1): 79-87. doi: https://doi.org/10.1016/0032-5910(93)85010-7.

Zeghal, M. and El Shamy, U. 2008. Liquefaction of saturated loose and cemented granular soils. *Powder Technology*, **184**(2): 254-265. doi: http://dx.doi.org/10.1016/j.powtec.2007.11.032.

Zhu, H.P., Zhou, Z.Y., Yang, R.Y. and Yu, A.B. 2007. Discrete particle simulation of particulate systems: Theoretical developments. *Chemical Engineering Science*, **62**(13): 3378-3396. doi: https://doi.org/10.1016/j.ces.2006.12.089.

Zou, Q. and He, X. 1997. On pressure and velocity boundary conditions for the lattice Boltzmann BGK model. *Physics of Fluids*, **9**(6): 1591-1598. doi: 10.1063/1.869307.